

# Experimental Study of Granular Material Flowability in a Heat Exchanger

Samkelo M. Khumalo <sup>1\*</sup> Daniel M. Madyira <sup>1</sup>, Waldemar F. Cieslakiewicz <sup>1</sup>, Dewald Scholtz <sup>2</sup>, Garikai T. Marangwanda <sup>1</sup>

<sup>1</sup>Department of Mechanical Engineering Science, University of Johannesburg, Johannesburg, South Africa

<sup>2</sup>DryTech International, Johannesburg, South Africa

**Abstract.** This paper presents an experimental investigation of granular material flowability in a heat exchanger. Spherical silicon particles are used as the granular materials in this study. The velocity profile created shows uneven particle velocity where particles towards the outlet flow faster with the velocity reaching 9.09 mm/s and the particles close to the wall flow slower with the velocity reaching 1.63 mm/s. Compared to the Carr classification of flowability proposed in the literature, the angle of repose obtained through the experiment, which is 15°, suggests that the particles are very free flowing. This is supported by the coefficient of rolling resistance which has been obtained as 0.001, suggesting that these particles have a lower rolling friction resistance, leading to a more efficient movement. Moreover, the mass flowrate implies that 140.85 grams of particles flow out per second. These findings suggest that particle size, outlet size, friction factors and the space between the heating elements and the walls affect the flowability of particles in the heat exchanger.

## 1 Introduction

Oran et al [1] define granular material as a collection of small solid particles that are closely packed and surrounded by fluid (typically gas). Additionally, Zhu et al [2] state that the particles demonstrate fluid-like behaviour as they adapt to the shape of their container, regardless of its geometry, they exhibit compressibility, can withstand deformation, and have the ability to flow and form heaps. As stated by Fernandes et al [3], the particles exist either in their natural state or as specialized materials designed for specific applications, such as additives and fillers in concrete, powdered food products, and fine-grain compact aggregates with high value-added uses in the chemical and pharmaceutical industries. Moreover, Tahmasebi [4] also emphasises that despite the advancements in experimental and computational techniques, our understanding of the physics of granular materials remains limited. For example [4], an estimate of 40% of the capacity is wasted in the industrial operations as a result of our lack of understanding of granular flowability. Traina et al [5] defines granular material flowability as the ability of the granular particles to flow consistently and regularly, making them well suited for mixing, processing and storage. Flowability of granular materials also depends on a set of other properties such as porosity [6], angle of repose [7], particle shape and size [8], particle surface roughness [9] and segregation capacity [5] just to name a few. A method called Carr classification of flowability, presented in Table 1, is used in powder technology to assess powder flowability. Based on this method of classification, an angle of repose lesser than 30° indicates free flowing material, while an angle greater than 55° indicates highly cohesive material [7].

**Table 1.** Carr classification of flowability based on angle of repose [7].

| Description                 | Repose | Angle    |
|-----------------------------|--------|----------|
| Very free flowing           |        | < 30°    |
| Free flowing                |        | 30 – 38° |
| Fair to passable flow       |        | 38 – 45° |
| Cohesive                    |        | 45 – 55° |
| Very cohesive (non-flowing) |        | > 55°    |

Rotating drums and vertically positioned hoppers play a crucial role in granular material flowability analysis. For instance, Zheng et al [10] have used rotating drum to study the flow behaviour of granular material using the Eulerian-formulation finite element method, where they observed a linear distribution of particle velocity along the mid-cord of the bed. Liu et al [11] have studied granular flow of bi-sized particles in a rotating drum that has gaps in the walls, using the discrete element method (DEM). In their study, one side of the wall is fixed while the other rotates. They observed that all small particles move towards the fixed end. The common findings when it comes to granular flow study in rotary drums is that researchers use analytical methods and not experimental methods, this is because experimental studies of rotating drums are often limited by difficulties in visualizing and measuring internal particle dynamics. On the other hand, vertically positioned hoppers allow for gravity-driven flow, making it easier to observe how particles behave in discharging systems.

Jian et al [12] have studied the flow characteristics of granular particles (with six different particles mainly plastic spheres, plastic cylinders, plastic cubes, wooden

\* Corresponding author: [samkelok746@gmail.com](mailto:samkelok746@gmail.com)

spheres, wooden cylinders, mug beans and their binary mixtures) experimentally in a flat-bottom hopper using high-speed, high-resolution camera recordings. The diameter of the particles ranged between 0.004 – 0.006 m, length of the cylindrical and cubic particles ranged between 0.005 – 0.0085 m, and densities between 476 – 1128 kg/m<sup>3</sup>. The study revealed that particle properties, such as shape and density, significantly influence their motion within the hopper. They also observed that the wooden cubic particles stack in the corner of the flat-bottomed hopper due to the friction between the particles. However, their study does not consider the effects of inclining the outlet and the wall friction of the discharge hopper.

Balevičius et al [13] and Balevičius et al [14] have studied granular flowability of spherical viscoelastic particles and pea grain with the same material properties having density of 500 kg/m<sup>3</sup>, Young’s modulus of 0.3 MPa, Poisson’s ratio of 0.3 and diameter ranging between 7.2–7.8 mm, in wedge-shaped hopper models. The wedge-hopper shapes included maximally inclined walls, transitional (with inclined walls with flat bottom) and vertical walls with flat bottom. Moreover, the outlet orifice size was kept constant for all hopper geometries. Their findings indicate that the flat-bottomed hoppers cannot be completely discharged as the particles form a stagnation region near the corners, which aligns with the findings from the study conducted by Jian et al [12]. They also observed that the wedge-shaped hopper with the maximum inclination angle demonstrates optimal discharge flow characteristics, aligning with the mass flow discharge mode. They conducted the same experiment with the space-wedged and plane-wedged hopper, having the geometrical parameters of B = 0.3 m, L = 1.6/2 m and H = 1.7 m. The space-wedged hopper is characterized by acute angles of  $\alpha_x = 68^\circ$  and  $\alpha_y = 62^\circ$ , whereas the plane-wedged hopper has angles of  $\alpha_x = 68^\circ$  and  $\alpha_y = 90^\circ$ . They also observed that the space-wedged hopper, compared to the plane-wedged hopper, exhibits lower outflow velocities and longer discharge times. The plane-wedged hopper allows for faster discharge due to its planar flow. The space-wedged hopper generates space-retarded flow. In such hoppers, particles dissipate their kinetic energy through contact, resulting in increased interaction among the particles and with their surroundings. However, this study only considers the discharge rates of the particles. They considered a specific number of particles into the hopper, they do not look at the flow profiles depicting the granular flow, to determine areas or regions of faster and slower flows.

## 2 Investigation Methodology

### 2.1. Aim

The aim of this paper is to study the flow behaviour of silicon granular particles in a heat exchanger manufactured from stainless steel using an experimental analysis.

### 2.2. Material Description

The experiments were conducted using spherical particles due to their well-defined geometry, which simplifies the flow behaviour. The experimental material consisted of uniform silicon spherical particles with a diameter of 4 mm, density of 2329 kg/m<sup>3</sup>, Young’s modulus of 112 GPa and Poisson’s ratio of 0.28. Prior to the experiment, particles were coloured with four different colours (mainly green, white, brown, and blue) to facilitate observation of the velocity profiles during particle flow. The uniform size, shape, and density of the spherical particles provided a controlled environment for analysing granular flow behaviour. The rolling resistance, angle of repose and static friction properties of the material had to be determined experimentally. The static friction of a particle is directly determined using the angle of repose, as demonstrated by Beakawi et al [7] and Aela et al [15]. The static friction coefficient is calculated using equation 1, which is derived by Beakawi et al [7].

$$\mu_s = \tan \vartheta \quad (1)$$

Where  $\mu_s$  is the coefficient of static friction and  $\vartheta$  is the angle of repose. To determine the angle of repose, an experiment was conducted in which particles were dropped into a cylindrical container from a specific height, forming a pile, as shown in Figure 1. In this study, the measured angle of repose was 15°. Through substitution into equation 1, the static friction coefficient of the particles becomes 0.268.



**Fig 1.** Angle of repose experiment (source: Drytech International (Pty) Ltd)

Zhu et al [16] define rolling resistance as the rolling friction that opposes the relative motion of particles. To determine this friction factor, an experiment was conducted, as depicted in Figure 2. In this experiment, a 1319 mm long 2205 stainless steel angle iron rod is positioned at an angle of 2.7°, as shown in Figure 2. A silicon particle is released from rest on one side of the rod and left to roll down its length. The time taken to complete the rolling is measured and the experiment is repeated 10 times for accuracy. The averaged time taken to complete the rolling is 11.6 seconds.

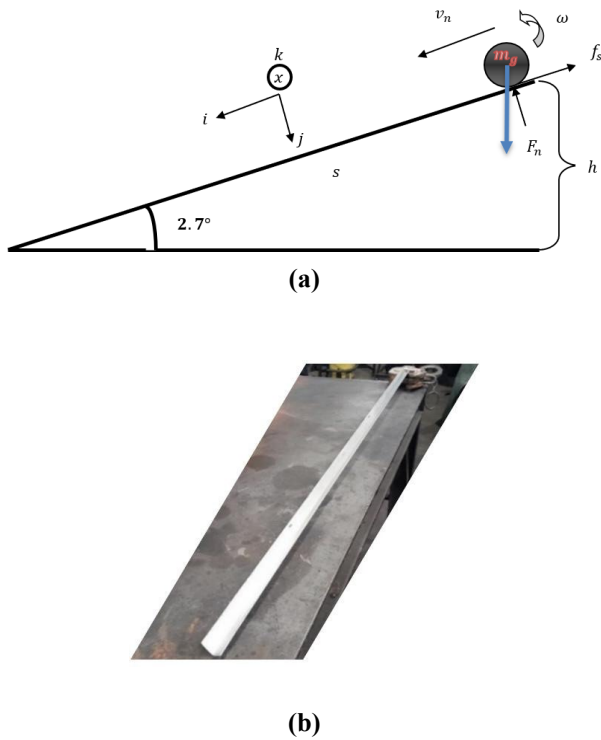


**Fig.2.** Rolling resistance experiment: (a) a schematic presentation of forces experienced by the particle when rolling; (b) rolling experiment set up (source: Drytech International (Pty) Ltd)

Through the application of the kinematic equations, the acceleration of the particle is obtained as 0.0196 m/s<sup>2</sup>. Applying Newton’s second law of motion, the torque method for the system as well as the moment of inertia of the particle, the rolling resistance expression reduces to equation 2.

$$\mu R = a / (2g \cos \theta) \quad (2)$$

Where  $\mu R$  is the rolling resistance coefficient of friction,  $a$  is the acceleration of the particle,  $g$  is the gravitational acceleration and  $\theta$  is the inclination angle of the angle iron rod. Therefore, the rolling resistance becomes 0.001. This lower rolling resistance coefficient implies that the particle has a lower rolling friction, leading to a smoother movement. This value aligns with the study conducted by Zhu et al [2], who studied monodisperse spherical particles with a diameter of 3 mm and density of 2500 kg/m<sup>3</sup>.

### 2.3. Equipment Description

The equipment setup comprised a heat exchanger, a tape measure and a digital camera. The heat exchanger was constructed from 2205 stainless steel material, with an overall length of 430 mm, depth of 80 mm, and width of 200 mm. The outlet of the heat exchanger is adjustable; however, for this study it was fixed at 80 by 8.8 mm. One of its walls is made of glass to facilitate the observation of particle flowability for easy measurement of particle velocity. The mechanical properties for stainless steel and glass are presented in Table 2. The heat exchanger has five obstacle holes at different locations as shown in Figure 3, which represent where the heating elements will be located. A tape measure is placed on the glass side as shown in Fig 3b, which is used to measure the distance travelled by a particle between two points. In this setup, the heat exchanger is fixed on supporting rods in such a way that there is enough space between the outlet and the platform where granular particles are discharged into. The flowability process of particles through the heat exchanger is solely gravity driven, where particles are allowed to freely discharge under gravity.

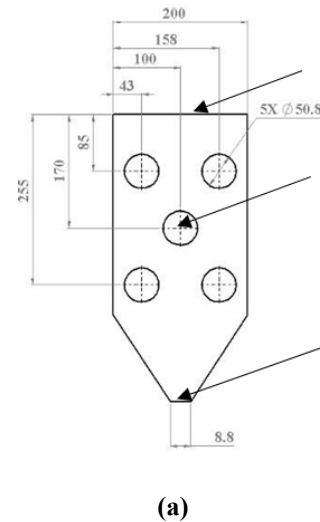


**Fig 3.** Heat exchanger: (a) dimensions; (b) test rig (source: Drytech International (Pty) Ltd)

**Table 2.** 2205 stainless steel [17] and glass [18], [19] mechanical properties.

| Properties                   | Value |
|------------------------------|-------|
| <b>2205 stainless steel</b>  |       |
| Density (kg/m <sup>3</sup> ) | 7800  |
| Young's modulus (GPa)        | 200   |
| Poisson's ratio              | 0.3   |
| Static friction coefficient  | 0.32  |
| <b>Glass</b>                 |       |
| Density (kg/m <sup>3</sup> ) | 2200  |
| Young's modulus (GPa)        | 0.094 |
| Poisson's ratio              | 0.22  |
| Static friction coefficient  | 0.162 |

The number of particles the heat exchanger can contain is determined by considering the heat exchanger volume, the volume of each particle, and the packing density fraction. According to Kallus [20], spherical particles that have uniform size have a packing density of about 64%, while Hao [21] estimates it to be approximately 63% for dense random packing. Assuming that the heat exchanger is a triangular prism and disregarding the empty spaces to be fitted with the heating elements and the triangular parts on the bottom half of the heat exchanger, its volume is determined to be 5075028.03 mm<sup>3</sup>, and the volume of a single spherical silicon particle with a diameter of 4 mm is determined to be 33.51 mm<sup>3</sup>. To calculate the number of particles, equation 3 is used.

$$n = (V_t \times \eta) / V_p \quad (3)$$

Where n is the number of particles, V<sub>t</sub> is the total volume of the heat exchanger, η is the packing efficiency and V<sub>p</sub> is the volume of an individual particle. For this study, the packing efficiency was based on Hao [21] as 63% as an assumption since the particles are randomly packed. Therefore, the number of particles that the heat exchanger can carry is 95 413 particles.

## 2.4. Experimental Description

The experiment was conducted in the order of determining the particle flow profile, particle velocity and mass flow rates. The following procedure was followed to investigate the flow characteristics of granular materials.

### 2.4.1. Particle flow profile experimental procedure

The heat exchanger was filled with differently coloured particles with the outlet closed. The outlet was then opened to initiate particle flow while the camera was set to record the flow behaviour. The trials were repeated three times for accuracy.

### 2.4.2. Particle velocity experimental procedure

Using the video recording, four different regions across the heat exchanger are selected to measure velocities of the particles. Figure 4 shows the selected regions, named from a to d. The white line presents the distance that the particle travels. The distance travelled was easily determined using a tape measure positioned alongside the glass. The time taken for the particle to travel between the points was recorded.

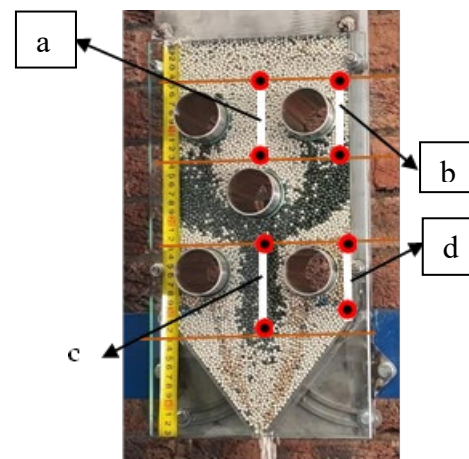


**Fig 4.** Granular particle flow measurement regions (source: Drytech International (Pty) Ltd)

The observed particle was allowed to travel between two points marked by red dots, with the upper dot designated as the initial point (P1) and the lower dot as the final point (P2). Table 3 provides the naming conventions for symbols representing different regions.

**Table 3.** Naming of different regions for velocity measurements

| Symbol | Name   |
|--------|--|
| a      | Region between two top tubes                     |
| b      | Region between the top right tube and the wall   |
| c      | Region between the two lower tubes               |
| d      | Region between the lower right tube and the wall |

### 2.4.3. Mass flow experimental procedure

The heat exchanger was filled with particles, which are then allowed to discharge while the time taken for discharge was recorded. Three sets of experiments were conducted, each consisting of five runs for accuracy. The discharged particles were weighed, and their mass was recorded alongside the time taken for the discharge.

### 3 Results and Discussions

Observations showed that particle flow rates vary and are not uniform across the heat exchanger. Figure 5 shows that particles flow faster towards the centre of the heat exchanger and slower towards the walls. Particle velocity decreases towards the walls because of friction and wall interactions. Slower flows are also caused by particles clogging between the heating elements and the side walls because of small space to let particles through. For easy observation, particles are injected into the heat exchanger in a certain order, in a way of varying colours. From Figure 5a, a blue line of particles separates the white and the brown coloured particles. However, when the particles start flowing, it is observed that from Figure 5a to Figure 5d, some of the blue particles remain at the bottom of the heating elements. This observation indicates that there is a stagnation region below the heating elements where particle flow is the slowest.

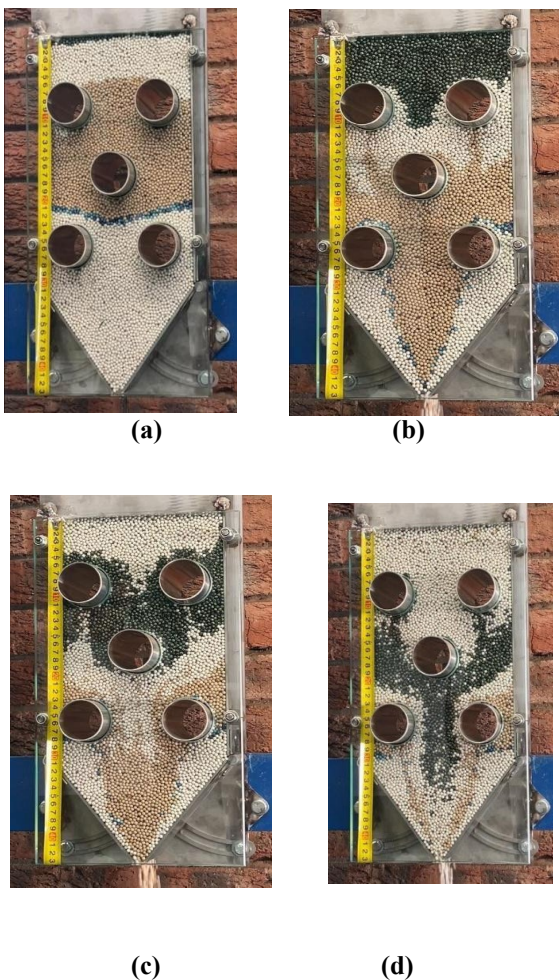


**Fig 5.** Particle flow in heat exchanger (source: Drytech International (Pty) Ltd): (a) initial phase before the outlet is opened; (b) flowing phase where particles make way to the outlet; (c) shows the general flow trend; (d) depicts a clear indication of fast and slow flow regions.

Another key parameter in granular flow dynamics is the particle flow velocity. This parameter provides

insight into particle flowability. The velocity profile has already revealed a non-uniform distribution, with maximum velocities occurring at the centre of the heat exchanger and significantly reducing towards the walls. Following the particle velocity experimental procedure, the total distance travelled by a particle is the difference between P1 and P2 and is used to calculate the velocity. The travelled distance by the particle and the time for the travel are presented in Table 4.

**Table 4.** Particle velocity at different regions within the heat exchanger

| Region | L(mm) | Time (s) | Velocity (mm/s) |
|--------|-------|----------|-----------------|
| a      | 82    | 12       | 6.83            |
| b      | 82    | 15       | 5.47            |
| c      | 100   | 11       | 9.09            |
| d      | 70    | 43       | 1.63            |

$$v = L / t \quad (4)$$

Where  $v$  is the particle velocity,  $L$  is the total distance travelled by a particle between two points ( $L = P1 - P2$ ) and  $t$  is the time taken by the particle to travel between two points.

The mass flow rate of the particles is determined through three sets of experiments, each consisting of five runs to enhance accuracy. Table 5 provides the average weight, discharge time, and mass flow rate of particles through the heat exchanger.

**Table 5.** Averaged weight and flow time for different experiments

| Experiment | Average mass (g) | Average flow time (s) | Average mass flowrate (g/s) |
|------------|------------------|-----------------------|-----------------------------|
| 1          | 4398.27          | 30.83                 | 142.65                      |
| 2          | 3951.96          | 28.1                  | 140.64                      |
| 3          | 3950.72          | 28.4                  | 139.11                      |

The average mass flow rate of the particles is calculated using equation 5 as follows:

$$\dot{m} = m_{av} / t_{av} \quad (5)$$

Where  $\dot{m}$  is the average mass flow rate of the particles in the heat exchanger,  $m_{av}$  is the average mass obtained through each experiment and  $t_{av}$  is the average time taken for the particles to be discharged from the heat exchanger. The average mass flow rate across the three experiments is 140.85 g/s. This indicates that 140.85 grams of 4 mm diameter silicon particles exit the heat exchanger per second through an outlet measuring 8.8 mm by 80 mm.

Particles are allowed to freely discharge under gravity. However, the experiment demonstrated that the velocity of the particles inside the heat exchanger is not uniform. As presented in Figure 5d, particles flow

faster through the centre and slower towards the walls of the heat exchanger. Gravity acts uniformly on all particles, but its effect is more pronounced in the central region because of a direct path to exit, thereby allowing particles at the centre to experience less resistance when compared to the particles near the walls. Table 4 shows that region c has fast flowing particles with velocity as high as 9.09 mm/s, followed by region a having velocity up to 6.83 mm/s, and the slowest being region d having particles flowing with the velocity of 1.63 mm/s. The mass flow rate of 4 mm diameter silicon particles through the heat exchanger with an outlet size of 8.8 mm has been obtained to be 140.85 g/s. In this study, the flowability of the particles is influenced by gravity and the size of the outlet. The angle of repose was measured to be 15°. Based on the Carr classification of flowability [7] presented in Table 1, the material under this study is classified as very free flowing. This is further supported by the calculated rolling resistance coefficient of 0.001, which typically implies smoother rolling.

## 4 Conclusions

In this study, granular material flowability in a heat exchanger has been analysed through experiments. In the experiment, the particles fall through the heat exchanger under the influence of gravity. The results revealed that the particle velocity is not uniform throughout the heat exchanger, with velocity profiles peaking at the centre of the heat exchanger and decreasing toward the walls. The results have also revealed that the size of the outlet affects the mass flow of the particles, meaning that increasing the size of the outlet will result in more particles flowing out of the heat exchanger. Moreover, in this experimental analysis, it has been shown that 4 mm diameter silicon particles are very flowable, which aligns with the Carr classification of flowability [7] when comparing the angle of repose. A smaller coefficient of rolling resistance also implies that particles will roll smoothly with reduced energy dissipation. To increase the flowability of the particles, one may increase the size of the outlet, reduce the particle size or introduce an external force to push the particles through the heat exchanger. These findings may be used for heat exchanger design optimization. Furthermore, the study was limited to a single-material experiment with uniform density, shape and size. Future research should investigate the effects of particle mixtures, different shapes, sizes and external forces to expand upon these results.

**Funding:** This research was funded by University of Johannesburg and DryTech International.

## References

1. E. S. Oran and J. P. Boris, Fluid dynamics, in Encyclopaedia of Physical Science and Technology (Third Edition), Third Edit., R. A. Meyers, Ed., Academic Press, New York, 31–43, (2002).
2. H. P. Zhu and A. B. Yu, Averaging method of granular materials, *Physical Review E – Statistical Physics, Plasmas, Fluids, and Related Interdisciplinary Topics*, **66**(2), 1, (2002).
3. S. Fernandes, H. C. Gomes, E. M. B. Campello, and P. M. Pimenta, A fluid–particle interaction method for the simulation of particle-laden fluid problems, *Proceedings of the XXXVIII Iberian Latin American Congress on Computational Methods in Engineering*, (2017).
4. P. Tahmasebi, A state-of-the-art review of experimental and computational studies of granular materials: Properties, advances, challenges, and future directions, *Progress in Materials Science*, **138**, 101157, (2023).
5. K. Traina, R. Cloots, S. Bontempi, G. Lumay, N. Vandewalle, and F. Boschini, Flow abilities of powders and granular materials evidenced from dynamical tap density measurement, *Powder Technology*, **235**, 842–846, (2013).
6. N. Stanley-Wood, Bulk powder properties: Instrumentation and techniques, in *Bulk Solids Handling: Equipment Selection and Operation*, pp. 1–67, (2009).
7. M. Beakawi Al-Hashemi and O. S. Baghabra Al-Amoudi, A review on the angle of repose of granular materials, *Powder Technology*, **330**, 397–417, (2018).
8. D. McGlinchey, *Bulk Solids Handling: Equipment Selection and Operation*, Blackwell Publishing Ltd, (2008).
9. P. Zhang, Zhongnan Bi, Hongyao Yu, R. Wang, Guangbao Sun, and Shaoming Zhang, Effect of particle surface roughness on the flowability and spreadability of Haynes 230 powder during laser powder bed fusion process, *Journal of Materials Research and Technology*, **26**, 4444–4454, (2023).
10. Q. J. Zheng and A. B. Yu, Modelling the granular flow in a rotating drum by the Eulerian finite element method, *Powder Technology*, **286**, 361–370, (2015).
11. X. Liu, W. Ge, Y. Xiao, and J. Li, Granular flow in a rotating drum with gaps in the side wall, *Powder Technology*, **182**(2), 241–249, (2008).
12. B. Jian and X. Gao, Investigation of spherical and non-spherical binary particles flow characteristics in a discharge hopper, *Advanced Powder Technology*, **34**(5), 104011, (2023).
13. R. Balevičius, R. Kačianauskas, Z. Mroz, and I. Sielamowicz, Discrete element method applied to multiobjective optimisation of discharge flow parameters in hoppers, *Structural and Multidisciplinary Optimisation*, **31**(3), 163–175, (2006).
14. R. Balevičius, R. Kačianauskas, R. Mróz, and I. Z. Sielamowicz, Analysis and DEM simulation of granular material flow patterns in hopper models of different shapes, *Advanced Powder Technology*, **22**, 226–235, (2011).
15. Aela, L. Zong, M. Esmacili, M. Siahkouhi, and G. Jing, Angle of repose in the numerical modeling of ballast particles focusing on particle-dependent

- specifications: Parametric study, *Particuology*, 65, 39–50, (2022).
16. H. P. Zhu and A. B. Yu, the effects of wall and rolling resistance on the couple stress of granular materials in vertical flow, *Physica A: Statistical Mechanics and its Applications*, 325(3–4), 347–360, (2003).
  17. F. Ben Saada, K. Elleuch, and P. Ponthiaux, On the tribocorrosion responses of two stainless steels, *Tribology Transactions*, 61(1), 53–60, (2018).
  18. I. Ishibashi, C. Perry, and T. K. Agarwal, Experimental determinations of contact friction for spherical glass particles, *Soils and Foundations*, 34(4), 79–84, (1994).
  19. Zeynep Yeşim İlerisoy and Burcu Buram Çolak, Discovery of innovative materials in structural system design: Glass structures, *Most Recent Studies in Science and Art*, 1225–1237, (2018).
  20. Y. Kallus, The random packing density of nearly spherical particles, *Soft Matter*, 12(18), 4123–4128, (2016).
  21. T. Hao, Viscosities of liquids, colloidal suspensions, and polymeric systems under zero or non-zero electric field, *Advances in Colloid and Interface Science*, 142(1–2), 1–19, (2008).